

# On the shrink-fit induced multiaxial stress state in adjacent notched shaft geometries

E. Leidich, S. Hofmann and B. Brůžek

Department of Engineering Design, Chemnitz University of Technology, Reichenhainer Str. 70, 09126 Chemnitz, Germany, E-mail: hofmann.stefan@mb.tu-chemnitz.de

**ABSTRACT.** *In this theoretical study, the influence of the shrink-fit on the stress state in two different adjacent notched shaft geometries is exemplified on the interference and the coefficient of friction. Both parameters were varied on a bending load in finite element analyses. It is shown that the investigated parameters conspicuously affect the mean stress and also the stress amplitude in the adjacent notches. Furthermore, the fatigue strength was evaluated by the local stress method (FKM-Guideline) for the material 1.0503 and compared with experimental results. The range of the degree of utilisation is presented subject to the analysed parameters. Differences between the numerical and experimental results are discussed.*

## INTRODUCTION

The changing cross-sections in shafts, as a result of load distribution and functionality, normally cause a multiaxial stress state. Often, two or more notches are close to each other. In this case, a superposition occurs and a mutual interaction of stresses and strains results. Typical applications are gear wheels or bearing rings in combination with a shaft shoulder. The nominal stress approach, can be used in high cycle fatigue (HCF) for shafts and axles, is inconvenient for the solution of this type of problem because mean stresses arise from the interference are not included in the nominal stress approach. Local concepts account more for the influence of contact properties on the stress state.

The shrink-fit parameters significantly influence the stress state of an adjacent notch. The mean stress is mainly influenced by the interference, for example in [1]. In addition, the contact behaviour of the shrink-fit is strongly determined by the coefficient of friction. The coefficient of friction again is dependent upon several parameters for example the material combination and the cyclic slip range. Thus different states, for instance gripping or slipping, can occur and affect the multiaxial stress state. Furthermore, the coefficient of friction is *trainable* to  $\mu = 1$  and higher over time [2]. The applied static pressure load and the rotating bending load cause a proportional ratio of stress amplitudes and a non-proportional ratio of mean stresses with constant principal stress directions.

In this study, the influence of the interference in combination with the coefficient of friction in the shrink-fit on the mean stress and on the cyclic stress amplitude has been

investigated theoretically for two different notches. Numerically determined local stresses are used to estimate fatigue strength with the Analytical Strength Assessment (FKM-Guideline) [3] for the material 1.0503. Experimental results from these two geometries with rotating bending, determined in [4], are compared and discussed with the theoretical results.

## MODEL GEOMETRIES

The research was focused on two types of shaft notches, (1) the fillet shaft shoulder ( $r = 4$  mm) and (2) the shaft shoulder with an undercut ( $r = 0.6$  mm). The geometry, presented in Figure 1, was selected on the basis of prior experimental analyses [4] of shaft-hub-connections.

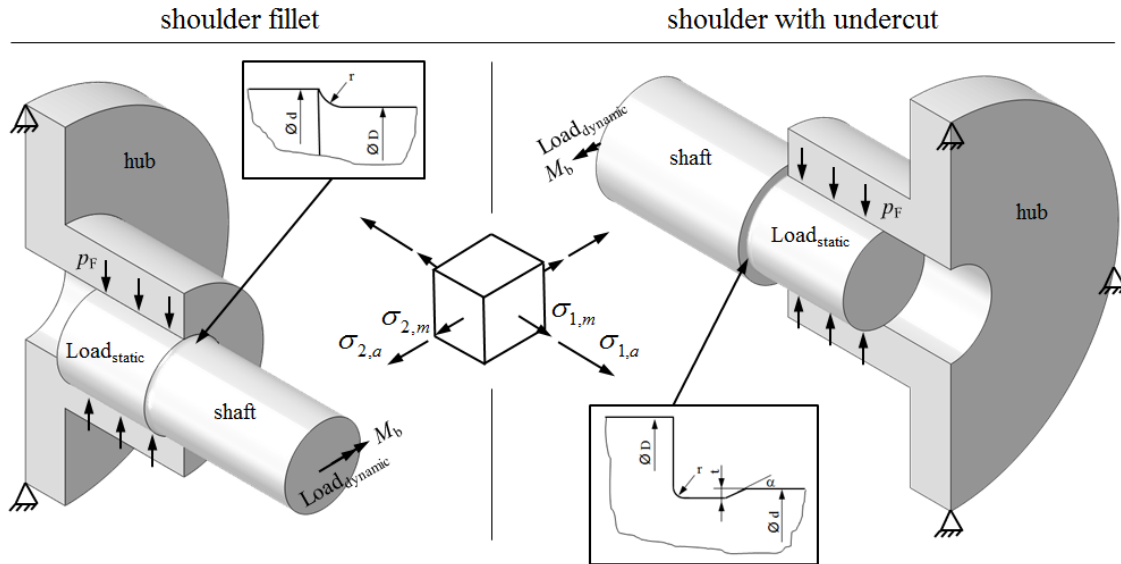


Figure 1. The two model geometries investigated in this work.

The geometry parameters of the shrink-fit connections are shown in Table 1, where  $Q_A$  is the ratio of the contact-diameter to the outside diameter of the hub. The definitions of absolute interference  $U$  and relative interference  $\xi$  are shown below (Equations 1 and 2). The interference  $U$  subjected to the diameter ratio  $Q_A$  and the Young's modulus  $E$  cause a contact pressure in the join. The nominal pressure  $p_F$  can be determined by Equation 3 according to the plain stress theory. Because of the singularity of the contact edge on the hub the pressure at this point is theoretically infinite, so the element length in the elastic numerical simulation determines the size of the contact pressure.

Table 1. Notch and shrink-fit parameters.

	shoulder fillet	shoulder undercut
contact diameter $d$ [mm]	40	40
shaft diameter $D$ [mm]	38.1	48
diameter ratio $d/D$	1.05	0.83
depth undercut $t$ [mm]	-	0.3
angle undercut $\alpha$ [°]	-	15
radius notch $r$ [mm]	4	0.6
diameter ratio $Q_A$	0.5	0.5

$$U = d_{shaft} - d_{hub} \quad (1)$$

$$\xi = \frac{U}{d} \quad (2)$$

$$p_F = \xi \cdot E \cdot \frac{1 - Q_A^2}{2} \quad (3)$$

## NUMERICAL ANALYSES

Numerical simulations were completed using a commercial finite-element code, *Abaqus 6.10-3*. Linear elastic material behaviour was assumed ( $E = 210,000$  MPa,  $\nu = 0.3$ ). First order elements C3D8R and C3D8I were used. For the contact properties in normal and tangential directions, the *penalty* approximation method [5] was chosen. The meshed shafts of the two geometries are shown in Figure 2.

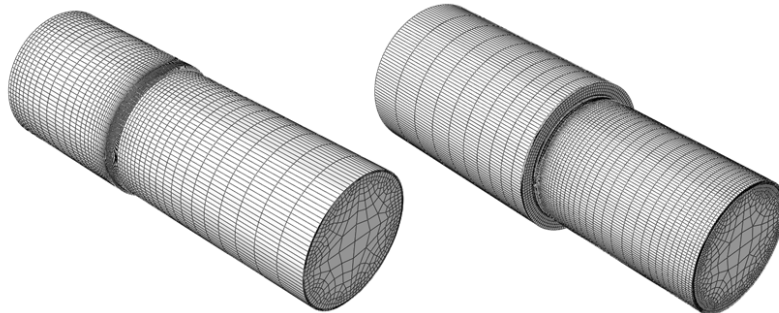


Figure 2. Meshed shafts of the two investigated shrink-fit geometries. Left: shaft shoulder fillet. Right: shaft shoulder with undercut.

The numerical simulations were carried out in two steps; the first is the contact step for the generation of the interference and the second is the load step with the applied bending moment. The interference between shaft and hub and the coefficient of friction in the area of contact were varied as follows:

- related interference  $\xi$  [%]: 0.5, 1.0 and 2.0
- coefficient of friction  $\mu$ : 0.1, 0.2, 0.4, 0.6 and 1.0.

At the surface of the notches a biaxial stress state exists do to the geometry. The static contact pressure causes mean stresses in the axial and tangential directions. The bending moment determines the local stress amplitudes in the same directions. According to the ratio between the static and the dynamic load, a non-proportionate synchronous ratio between the mean stresses and the stress amplitudes occurs. Figure 3 presents the biaxial stress ratio  $\sigma_2/\sigma_1$  for both geometries for one load case. It is shown that these ratio depends on the coefficient of friction.

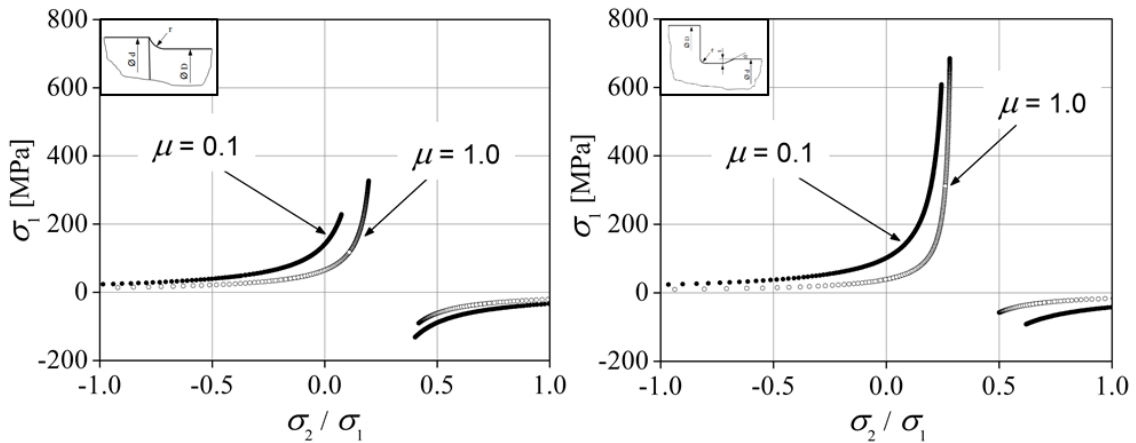


Figure 3. Biaxial stress ratio;  $\sigma_{nom,a} = 100$  MPa,  $\xi = 2.0$  ‰. Left: shaft shoulder fillet. Right: shaft shoulder with undercut.

The results of the numerical investigations are illustrated in Figures 4 and 5. The analyses were carried out on the point of both notches with the highest local stresses. This point correlates with the experimental failure position. The coefficient of friction and the interference have a considerable influence on the stiffness and the slip range in the area of contact and thus also on the stress state in the adjacent notch. Generally a greater coefficient of friction causes a larger stress concentration factor. There is an approx. 10% difference in stress amplitudes between the smallest and largest coefficient of friction in both geometries.

The mean stress is clearly influenced by the interference. But the coefficient of friction also has a significant effect on the mean stress value. The difference in mean stress can be up to 40% between the smallest and largest coefficient of friction.

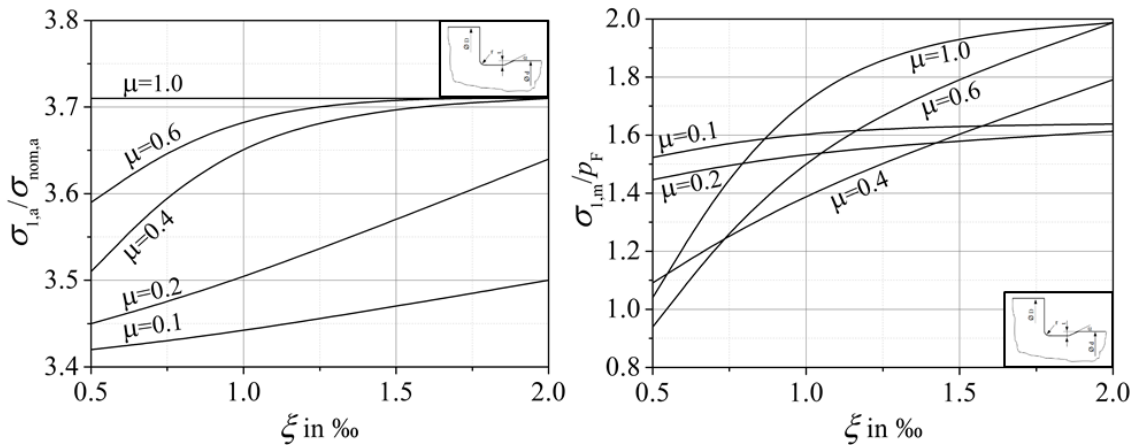


Figure 4. Influence of the coefficient of friction on the stress amplitude (left) and mean stress (right); *undercut shaft shoulder*.

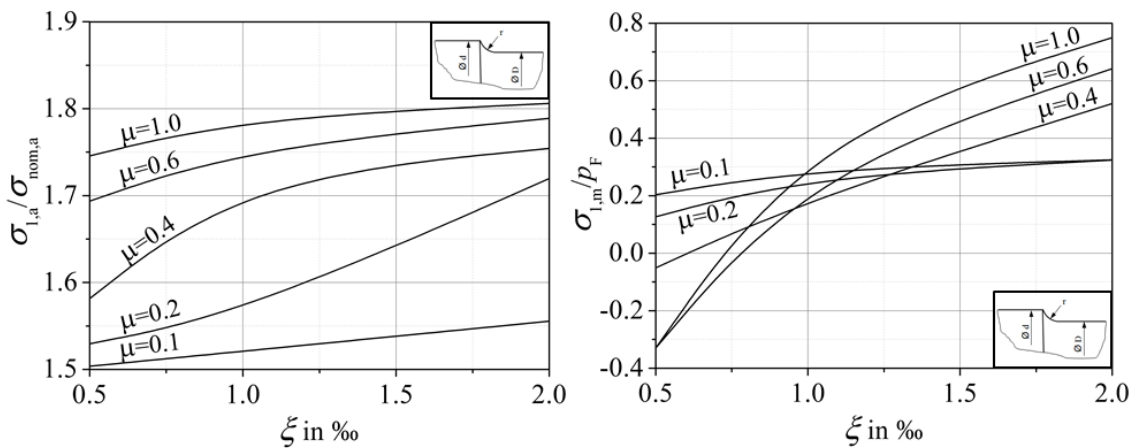


Figure 5. Influence of the coefficient of friction on the stress amplitude (left) and mean stress (right); *fillet shaft shoulder*.

## LOCAL STRESS METHOD

An appropriate procedure for the determination of the fatigue life or fatigue strength is the local stress method. Among others it is implemented in the Analytical Strength Assessment (FKM-Guideline), a guide for the dimension of mechanical components.

Based on the material strength, the fatigue strength of components is determined by taking into account a number of strength reducing parameters for example stress gradients or the mean stress. By means of a safety factor, a degree of utilisation can be calculated for the assessment; it is also possible to calculate this for variable loading.

In this study the FKM-Guideline is used to calculate the fatigue strength of both geometries for the material 1.0503, based on the local stresses according to the interference and the coefficient of friction. The component fatigue limit for completely reversed stress  $\sigma_{WK}$  (Equation 4) is defined by the material fatigue limit for completely reversed stress  $\sigma_W$ , which was determined experimentally [4] and the design factor  $K_{WK}$ .

$$\sigma_{WK} = \frac{\sigma_W}{K_{WK}} \quad (4)$$

Thereby the design factor is calculated as follows (Equation 5):

$$K_{WK} = \frac{1}{n} \cdot \left( 1 + \frac{1}{\tilde{K}_f} \cdot \left( \frac{1}{K_R} - 1 \right) \right) \quad (5)$$

Stress gradients are considered in Equation 6. The terms  $a_G$  and  $b_G$  are material constants and have the value 0.5 and 2700 in the case of material 1.0503.

$$n = 1 + \sqrt[4]{\bar{G}} \cdot 10^{-\left(a_G + \frac{R_m}{b_G}\right)} \quad (6)$$

The component fatigue strength  $\sigma_{AK}$  as a function of mean stress  $\sigma_m$ , mean stress sensitivity  $M$  and stress ratio  $R$ , described in the *Haigh-diagram*, is defined by the mean stress factor  $K_{AK}$  (Equation 7).

$$\sigma_{AK} = K_{AK} \cdot \sigma_{WK} \quad (7)$$

Subsequently, the local stress amplitude  $\sigma_a$  is related to the component fatigue strength  $\sigma_{AK}$  and from this follows the degree of utilisation  $a_{AK}$ . This factor has to be calculated for each principal direction. A combined degree of utilisation  $a_{AK,V}$  is then calculated with the v. Mises criterion as follows (Equation 8):

$$a_{AK,V} = \sqrt{\frac{1}{2} \left[ (a_{AK,1} - a_{AK,2})^2 + (a_{AK,2} - a_{AK,3})^2 + (a_{AK,3} - a_{AK,1})^2 \right]} \quad (8)$$

For the numerical analyses a *trained* coefficient of friction  $\mu = 0.6$  was assumed. The material tensile strength  $R_m = 690$  MPa and the material fatigue limit  $\sigma_W = 280$  MPa come from experimental tests on un-notched specimens for the material 1.0503, removed and made from the shrink-fits. Other factors for the assessment of the two geometries are shown in Table 2.

The comparison between results of the local stress concept and the experimental results for the fillet shoulder shows a small non-conservative behaviour in contrast to the undercut shoulder, where the degree of utilisation is 20% higher and thus conservative.

Table 2. Factors for the assessment (FKM-Guideline) of the two geometries; the local stresses correlate with the experimental failure load ( $\sigma_{nom,a,fillet} = 159$  MPa,  $\sigma_{nom,a,undercut} = 108$  MPa,  $\xi = 1.7\%$ ,  $\mu = 0.6$ ).

factors	shoulder fillet		shoulder undercut	
	1	2	1	2
principal direction				
local stress amplitude $\sigma_a$ [MPa]	283	67	401	120
local mean stress $\sigma_m$ [MPa]	66	2	251	45
related stress gradient $\tilde{G}$ [mm <sup>-1</sup> ]	0.45	0.39	1.91	1.36
stress gradient factor $n$	1.12	1.11	1.21	1.19
roughness factor $K_R$	0.94	0.94	0.94	0.94
roughness notch factor $\tilde{K}_f$	2	2	3	3
design factor $K_{WK}$	0.92	0.93	0.85	0.86
mean stress sensitivity $M$	0.14	0.14	0.14	0.14
stress ratio $R$	-0.62	-0.94	-0.23	-0.45
mean stress factor $K_{AK}$	0.97	1.0	0.89	0.98
component fatigue limit $\sigma_{AK}$ [MPa]	294	301	295	320
degree of utilisation $a_{AK}$	0.96	0.22	1.36	0.38
combined degree of utilisation $a_{AK,V}$	0.87		1.21	

Furthermore, the degree of utilisation was determined with other theoretical contact parameters and the same bending load. It follows a range of utilisation, presented in Figure 6. For the analysed material the difference in utilisation can be up to 15% between the largest and smallest coefficient of friction. Higher strength materials or case hardened materials, for instance, have significantly higher mean stress sensitivity, so the effect of the coefficient of friction on the component strength is more pronounced.

Another point not considered in this study is the wearing process in the slip area. Wear may influence the stress state (mean stress) extra. Future investigations will determine experimentally the local strains due to the shrink-fitting and the dynamic bending load over time. If the stress and strain states change over time, it is conceivable that the calculations may be performed to take into account the damage accumulation.

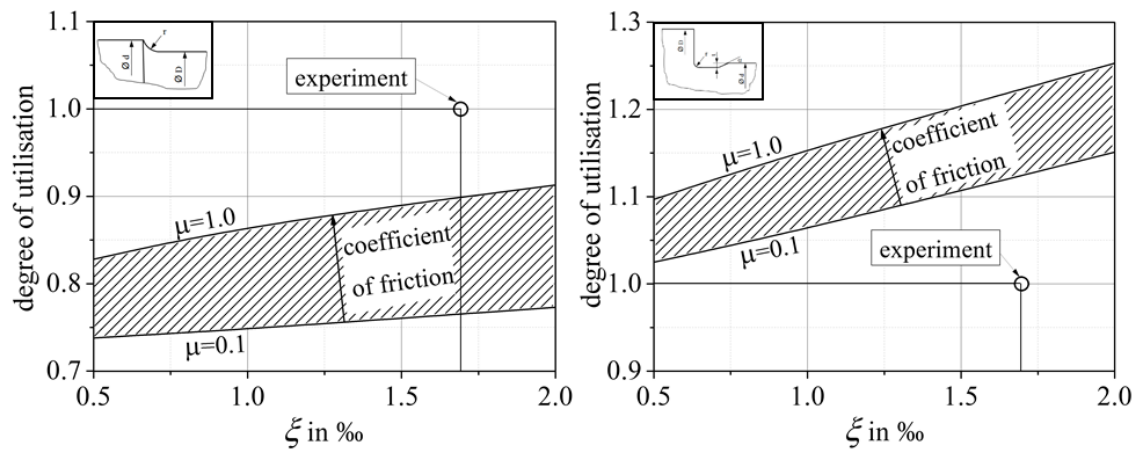


Figure 6. Degree of utilisation in the range between the smallest and largest coefficient of friction. Left: shaft shoulder fillet. Right: shaft shoulder with undercut.

## CONCLUSION

This study shows the influence of the interference and of the coefficient of friction in a shrink-fit on the stress amplitude and on the mean stress in an adjacent notch. Depending on the ratio of the static pressure load to the dynamic bending load, a lack of proportionality may exist between stress amplitudes and mean stresses. For the material 1.0503 the analytical results from the FKM-Guideline show a relative small deviation to the experimental results. A higher coefficient of friction leads to a more conservative strength assessment. The actual occurring mean stress in the load mode should be investigated experimentally for example with a strain measurement.

## REFERENCES

1. Leidich, E., Brůžek, B. (2010) *Proceedings of ICMFF10*, Parma.
2. Leidich, E., Maiwald, A., Vidner, J. (2012) *Wear* **297**, 903-910.
3. FKM-Guideline (2012) *Analytical Strength Assessment*, FKM e.V., Frankfurt.
4. Brůžek, B., Leidich, E. (2009) *FKM-Abschlussbericht* **305**.
5. Abaqus 6.10 *Documentation*.